Molecular Therapy
Original Article

Bioengineered AAV Capsids with Combined High Human Liver Transduction In Vivo and Unique Humoral Seroreactivity

Nicole K. Paulk,[1] Katja Pekrun,[1] Erhua Zhu,[2] Sean Nygaard,[3] Bin Li,[3] Jianpeng Xu,[1] Kirk Chu,[1] Christian Leborgne,[4] Allison P. Dane,[5] Annelise Haft,[3] Yue Zhang,[1] Feijie Zhang,[1] Chris Morton,[6] Marcus B. Valentine,[7] Andrew M. Davidoff,[6] Amit C. Nathwani,[8,9,10] Federico Mingozzi,[4,11] Markus Grompe,[3] Ian E. Alexander,[2] Leszek Lisowski,[2,12] and Mark A. Kay[1]

[1]Departments of Pediatrics and Genetics, Stanford University, Stanford, CA 94305, USA; [2]Translational Vectorology Group, Children's Medical Research Institute, University of Sydney, Sydney, NSW, Australia; [3]Oregon Stem Cell Center, Oregon Health & Science University, Portland, OR 97239, USA; [4]Genethon and INSERM U951, Evry, France; [5]Department of Haematology, UCL Cancer Institute, London, UK; [6]Department of Surgery, St. Jude Children's Research Hospital, Memphis, TN 38105, USA; [7]Cytogenetic Shared Resource, St. Jude Children's Research Hospital, Memphis, TN 38105, USA; [8]Department of Haematology, UCL Cancer Institute, London, UK; [9]Department of Haematology and Katharine Dormandy Haemophilia Centre & Thrombosis Unit, Royal Free London NHS Foundation Trust Hospital, London, UK; [10]National Health Services Blood and Transplant, Watford, UK; [11]University Pierre and Marie Curie, Paris, France; [12]Military Institute of Hygiene and Epidemiology (MIHE), Puławy, Poland

Existing recombinant adeno-associated virus (rAAV) serotypes for delivering in vivo gene therapy treatments for human liver diseases have not yielded combined high-level human hepatocyte transduction and favorable humoral neutralization properties in diverse patient groups. Yet, these combined properties are important for therapeutic efficacy. To bioengineer capsids that exhibit both unique seroreactivity profiles and functionally transduce human hepatocytes at therapeutically relevant levels, we performed multiplexed sequential directed evolution screens using diverse capsid libraries in both primary human hepatocytes in vivo and with pooled human sera from thousands of patients. AAV libraries were subjected to five rounds of in vivo selection in xenografted mice with human livers to isolate an enriched human-hepatotropic library that was then used as input for a sequential on-bead screen against pooled human immunoglobulins. Evolved variants were vectorized and validated against existing hepatotropic serotypes. Two of the evolved AAV serotypes, NP40 and NP59, exhibited dramatically improved functional human hepatocyte transduction in vivo in xenografted mice with human livers, along with favorable human seroreactivity profiles, compared with existing serotypes. These novel capsids represent enhanced vector delivery systems for future human liver gene therapy applications.

INTRODUCTION

Liver gene therapy research has progressed markedly over the last several decades. Although there has been substantial progress in treating patients with recombinant adeno-associated virus (rAAV) vectors expressing a transgene such as human Factor IX in hemophilia B,[1,2] relatively high doses of vector are required for a therapeutic response.[3,4] For non-cell-autonomous diseases like hemophilia that have the benefit of secreted elements, these low transduction levels may be sufficient when paired with transfer vectors optimized for high expression. However, such transduction levels will be suboptimal for liver diseases with more demanding cell-autonomous phenotypes. Numerous hurdles remain for improving long-term functional human liver transduction including increasing total functional hepatocyte transduction levels, pre-existing neutralizing antibodies (nAbs) against rAAV capsids, and cellular immune responses to capsid peptides presented on transduced hepatocytes. Current suboptimal transduction likely stems from the fact that, historically, preclinical rAAV selection and validation were performed in animal models that neither recapitulated human hepatocellular tropism nor the kinetics and strength of expression that can be reached.[1,5] Humoral neutralization of rAAV in the bloodstream arises from patient exposure to parental serotypes in nature.[6–11] Immune-mediated destruction of transduced hepatocytes is due to $CD8^+$ T cell responses to rAAV capsid components,[12] but this can largely be managed via corticosteroid administration[1] and reduced dosing. Thus, high-level, functional human hepatocyte transduction and evading humoral neutralization remain leading barriers to truly efficacious clinical liver gene therapy today.

Importantly, rAAV vectors can be bioengineered to achieve transduction and neutralization potentials not possible with parental serotypes through directed evolution of diverse capsid libraries.[13–15] Our

Received 27 March 2017; accepted 20 September 2017;
https://doi.org/10.1016/j.ymthe.2017.09.021.

Correspondence: Mark A. Kay, Departments of Pediatrics and Genetics, Stanford University, 269 Campus Drive, Stanford, CA 94305, USA.
E-mail: markay@stanford.edu

Table 1. Literature Comparison of Functional Hepatocyte Transduction and Pre-existing Neutralizing Antibody Levels in Humans with Existing Hepatotropic AAV Serotypes

AAV Serotype	Estimated Human Hepatocyte Transduction from Clinical Trials	Human Hepatocyte Transduction in Humanized Mice	Mouse Hepatocyte Transduction	Levels of Pre-existing nAb in Humans
AAV2	low[2]	low[4]	low[4,18,55]	medium[28,36] to high[9,10,28,29,35]
AAV3b	ND	low[4] to medium[3]	low[3,4,24,56]	high[9,29]
AAV5	low[57,58,a]	low[3]	low[3,18,24,59]	low[36,58,a] to medium[10,29,35,36] to high[29]
AAV8	low[1,5]	low[3,4]	medium[3] to high[4,60]	medium[28,35] to high[9,10,29]
AAV9	ND	low[3]	medium[3]	medium[35]
AAV-LK03	ND	high[4]	low[4]	medium[9]

The ability to functionally transduce hepatocytes in vivo in different settings was compared (we define a "functional" transduction event as one that expresses the payload, not vector copy numbers). Column 1 shows estimated functional percent human hepatocyte transduction from clinical trials. All values are estimates because no biopsies assessing functional transduction (protein expression rather than vector copy number) post-treatment have been performed. Of note, although expression levels from AAV8 were therapeutic in some patients (sustained 5%–7% of normal human *FIX* levels), previous data showing supraphysiological expression per transduced hepatocyte suggest <10% of patient hepatocytes were functionally transduced. Column 2 shows actual percent human hepatocyte functional transduction in vivo measured from treated xenografted liver mice. Column 3 shows actual percent mouse hepatocyte functional transduction in vivo from non-xenografted mice of varying genotypes and strain backgrounds. Column 4 compares estimated levels of pre-existing neutralizing antibodies (nAb) measured from human sera in neutralization assays (caveat: using various methodologies). ND, not determined.

[a]Predicted (data acquired from a non-peer-reviewed press release prior to the end of the study). For the three transduction columns, low = 0%–10%, medium = 10%–50%, and high = 50%–100% of hepatocytes. For the neutralization column, low = 0%–10%, medium = 10%–50%, and high = 50%–100% of patients whose sera showed neutralization for that AAV capsid.

technique utilizes replicating AAV throughout the entire selection and evolution process. In contrast to non-replicating screens that only select for receptor binding and uptake,[16,17] approaches that use replicating AAV select for every step in the intrahepatocellular trafficking and expression cascade, all of which can heavily influence the efficiency of transduction post-entry.[5,18–20] Of note, the Ad5 used to replicate the AAV library only replicates in human and not mouse cells.[13] This adds assurance that we are selecting AAVs capable of transducing human hepatocytes in the context of this xenograft model, where the only human cells present are human hepatocytes. Additionally, even single amino acid capsid mutations have been shown to affect functional transduction post-entry and post-uncoating.[21] Taken together, all these data support the use of replicating AAV screens whenever possible.

Here, we combined each of these important parameters: utilizing replicating AAV libraries that allow for selection beyond just hepatocyte receptor binding and entry, evolving human hepatocyte tropism in human rather than mouse hepatocytes in vivo, screening for humoral evasion against pools of human immunoglobulins from thousands of patients, and assessing transduction using clinically meaningful methodologies. The result is a panel of novel rAAV variants with higher levels of human hepatic transduction and unique humoral neutralization compared to previously characterized serotypes.

RESULTS

No Existing rAAV Serotype Fulfills All the Necessary Criteria for Ideal Liver Delivery in Humans

None of the current rAAV vector candidates in clinical development satisfies the combinatorial needs of high functional human hepatocyte transduction and low neutralization potential. Although several candidates have demonstrated detectable human hepatocyte transduction in either clinical trials or in xenograft models, none of those variants exhibit favorable neutralization profiles and vice versa (Table 1). Any rAAV that has not been tested in either a human liver trial or in humanized liver mice was excluded from this list, because assessing human hepatocyte transduction solely in cell lines (rAAV-F series[22]) or non-humanized mice (rAAV1[23,24]) often does not correlate with human liver transduction.[1,5]

Diverse AAV Capsid Library Screening in Primary Human Hepatic Xenografts In Vivo

To evolve new capsids with high functional hepatic transduction and immune-evasive properties, we employed a directed evolution approach that bioengineered diverse capsids through DNA shuffling of capsid genes from numerous genetically and functionally diverse parental AAV serotypes. Enzymatic fragmentation followed by assembly of shuffled full-length capsid genes was used to generate a diverse capsid library. Those were then cloned into an AAV shuttle vector and utilized to produce live replicating AAV libraries (Figure 1A). Our library was produced from 10 different parental capsid serotypes: 1, 2, 3b, 4, 5, 6, 8, 9_hu14, avian, and bovine. To maximize the likelihood that our shuffled capsids could both evade humoral neutralization and functionally transduce human hepatocytes, we performed multiplexed sequential screens using primary human tissues. First, primary human hepatocytes were transplanted into $Fah^{-/-}/Rag2^{-/-}/Il2rg^{-/-}$ (FRG)[25] mice using established protocols (Figure 1B). 5E10 vector genomes (vg) of the AAV library was administered intravenously (i.v.) into xenografted mice (Figure 1C), followed by i.v. injection of wild-type Adenovirus-5 (Ad5). AAV variants that successfully transduced and replicated in human hepatocytes were isolated 2 days post-Ad5 administration, minimally purified and re-titered, and again injected at 5E10 vg/mouse into another round of xenotransplanted mice. This in vivo screening cycle

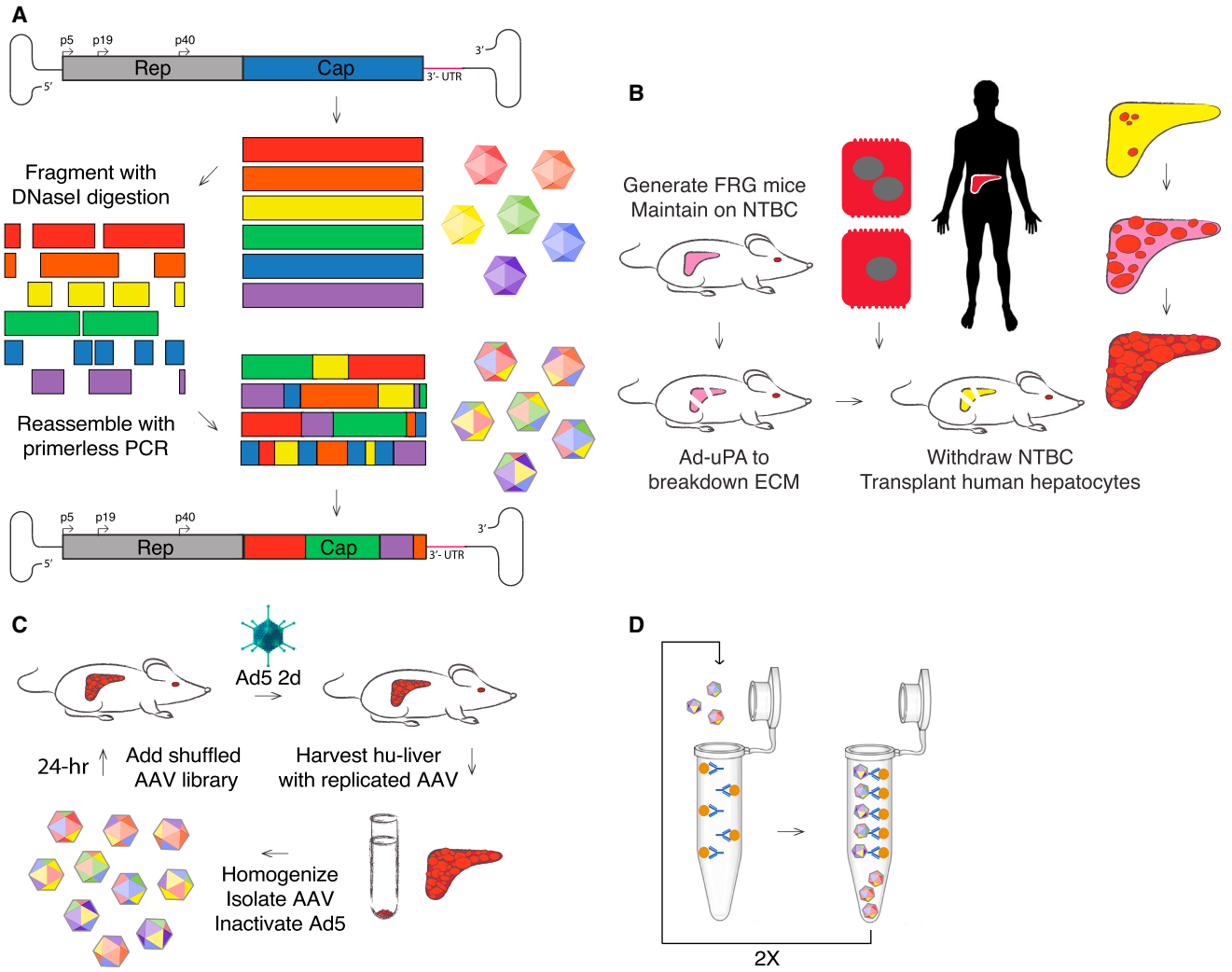

Figure 1. Directed Evolution of Adeno-associated Virus Capsids by DNA Shuffling and Multiplexed Sequential Screening in Humanized Liver Mice and against Pooled Human Immunoglobulins

(A) AAV capsid genes from 10 parental serotypes (1, 2, 3b, 4, 5, 6, 8, 9_hu14, avian, and bovine) were PCR-amplified, fragmented with DNase I digestion, and then randomly reassembled through self-priming PCR. Resultant shuffled *Cap* genes were cloned back into a replication-competent AAV production plasmid via flanking SwaI/NsiI sites downstream of AAV2 *Rep*. The resultant library production plasmid contained AAV2 ITRs and a modified AAV2 3′ UTR. The AAV library was packaged using standard production protocols, dot-blot titered and used for selection. (B) Diagram illustrating the procedure for producing humanized liver FRG mice with NTBC selection for selection in humanized liver mice. (C) Diagram illustrating the initial five-round selection screen with replicating AAV capsid libraries from (A) in humanized liver mice from (B). (D) Diagram illustrating the subsequent two-round subscreen against pooled human immunoglobulins with the evolved AAV library already screened for human hepatocyte tropism. Capsids that did not bind pooled human immunoglobulins were taken for further characterization.

was carried out for five rounds of selection. Diversity monitoring via Sanger sequencing began at round 3, and each round thereafter, until round 5 when human hepatic transduction had been selected, but some library diversity remained. This enriched human hepatotropic AAV library was then used as input for a series of sequential on-bead screens against pooled human immunoglobulins from thousands of patients to select variants with reduced humoral neutralization potential across the general population (Figure 1D). After two rounds of binding selection, those variants that remained unbound were subjected to stringent characterization for potential clinical utility.

Identifying Functionally Important Residues via Structural and Comparative Computational Modeling

At the completion of the second sequential screen, capsid sequences amplified from the input library and several selection rounds were deep sequenced using Pacific Biosciences (PacBio) single-molecule sequencing. Round-to-round positional analyses from thousands of

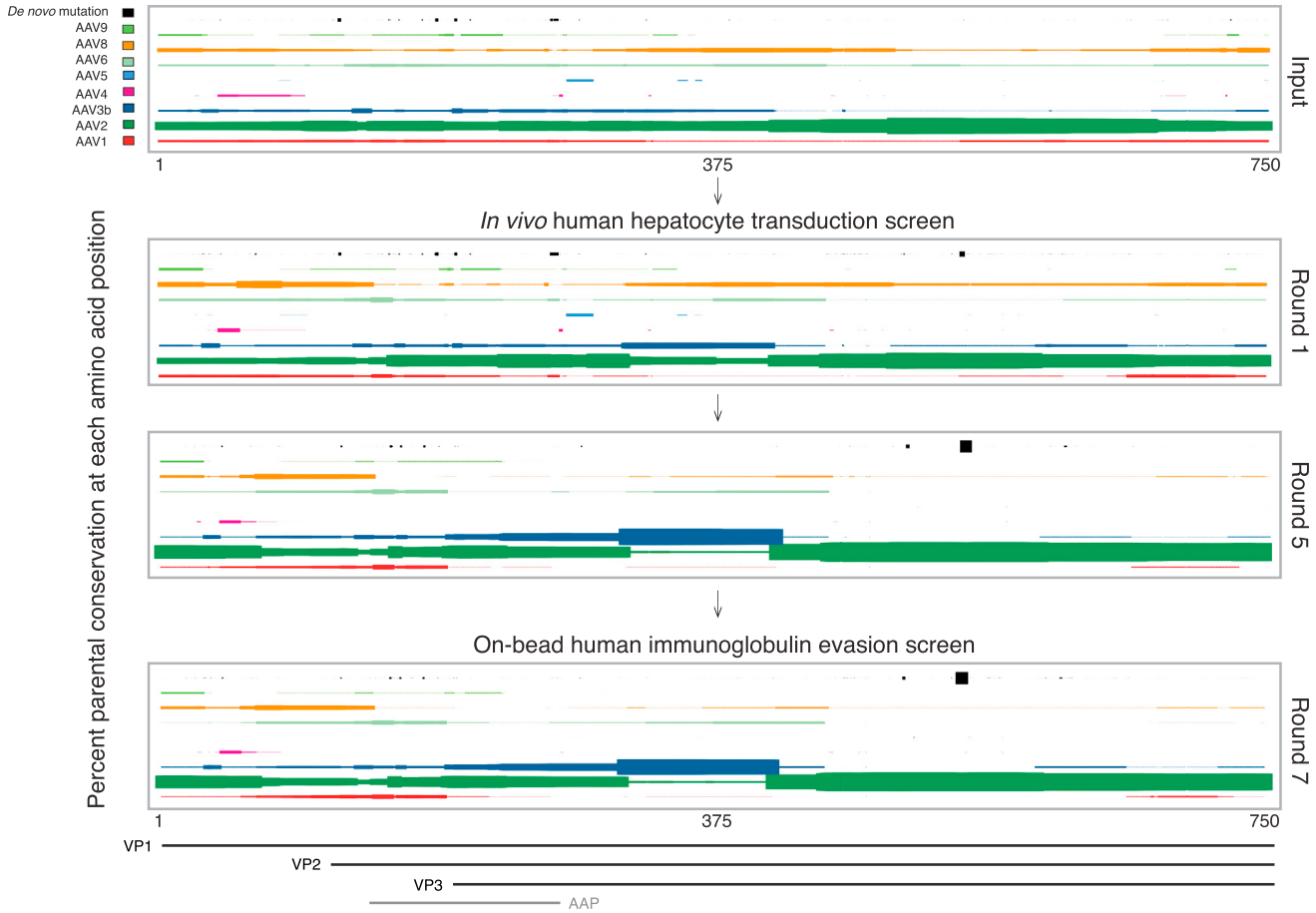

Figure 2. Percent Parental Conservation at Each Amino Acid Position during the Progression of Each Screen

Using PacBio single-molecule sequencing and bioinformatics analyses, positional enrichment assessments were performed to calculate percent conservation among amino acids from parental serotypes (AAVs 1, 2, 3b, 4, 5, 6, 8, and 9_hu14) or de novo mutations for each amino acid position among all capsids at key rounds during the screen. Bovine and avian were removed from the plot because few variants showed any appreciable contribution from those two serotypes. The maximum square size indicates that 100% of variants share that amino acid from that parent at that position. All other square sizes are proportional to the percent of variants from 0%–100% that have that amino acid at that position from that parent. Each parent is colored as is shown in the legend (same color scheme is used in Figures 3A and 3B), and de novo mutations that evolved during the screen are shown in black. VP1, VP2, VP3, and AAP ORFs are diagrammed below for reference.

capsids identified the selection for key residues (Figure 2). This approach was more revealing than classic phylogenetic trees that root on the nearest full-length parental sequence, effectively masking functionally important residues within full-length capsid relatedness (Figure S1). Interestingly, although rAAV2 is known to be a poor functional transducer of human hepatocytes, several structural fragments from AAV2 were highly selected in the initial screen during the early rounds of screening, most notably residues in the C-terminal end of VP3, where heparin sulfate proteoglycan (HSPG) binding residues reside (R585 and R588).[26] However, many stretches of AAV2 sequence were strongly selected against, including a portion of the unique region of VP1 and the unique region of VP2 (aligned residues 67–146), which instead selected for residues shared by AAVs 1/6/8; a large stretch of VP3 (aligned residues 321–423), which near exclusively selected for AAV3b residues; and several high-frequency de novo mutation hotspots (aligned residues 42, 158, 165, 181, 290, 515, and 555), which contained various amino acids not present in any of the parental serotypes used for library generation. As we transitioned into the second screen to select capsid variants capable of humoral evasion, the immunoglobulin G (IgG)-bound and unbound AAV variants exhibited a high degree of structural mean similarity. Only a few key regions were different between them that are likely necessary in combination to achieve the improved IgG evasion. Here, the global differences were more easily seen with the individual, rather than aggregate, full-length capsid sequences from PacBio single-molecule sequencing (Figure S1A).

To further probe the evolved variants, we chose six pools of the most highly selected capsid variants obtained after the final screen (Figure S2A) and vectorized them as pools with GFP for an additional IgG-binding assessment. The variants of the best-performing pool were then individually vectorized with GFP and Firefly Luciferase

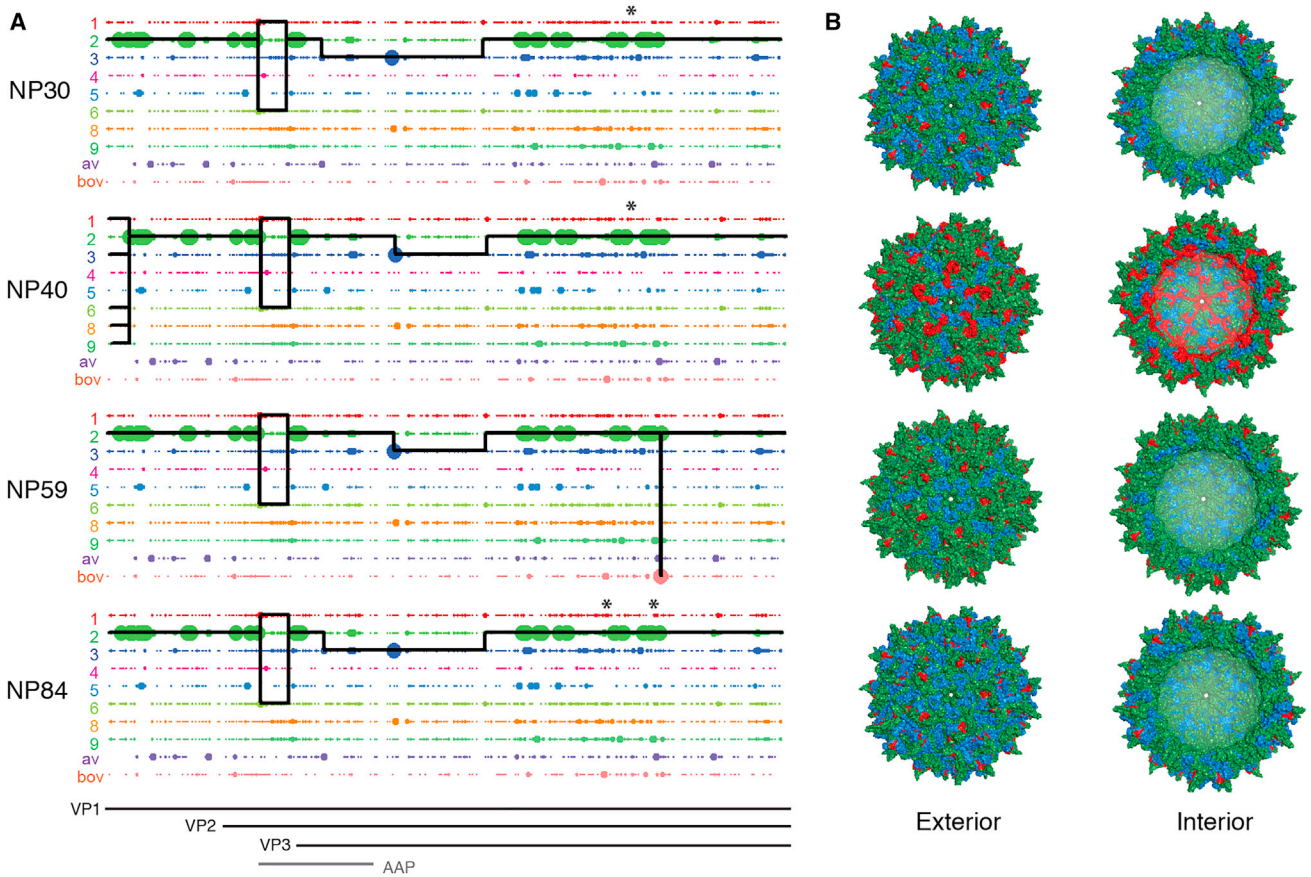

Figure 3. Sequence and Structural Composition of New Human Hepatotropic Shuffled AAV Capsid Variants

(A) Crossover mapping analysis of capsid fragment crossovers in vectorized variants from the parental AAV serotypes (AAVs 1, 2, 3b, 4, 5, 6, 8, and 9_hu14) used in the library. The maximum circle size indicates a 100% match for that amino acid from that parent at that position. All other circle sizes are proportional to the percent likelihood that that amino acid at that position matches that parent. The solid black line for each chimera represents the most likely parental serotype match identified across each crossover. Thin parallel lines between crossovers indicate multiple parental matches at an equal probability. Vertical spikes indicate a mutation from within the parental sequence space, while an overhead asterisk indicates an evolved de novo mutation for which no parent has that amino acid at that position. VP1, VP2, VP3, and AAP ORFs are diagrammed below for reference. (B) Shuffled variants were 3D false-color-mapped onto the crystal structure of AAV2. Color coding indicates parental contribution using the same colors as in (A).

(FLuc) expression constructs for subsequent validation experiments. Those capable of producing titers sufficient for eventual clinical use (variants NP30, NP40, NP59, and NP84) and excellent packaging ratios were considered further for validation (Figures S3A and S3B). To determine the genetic contribution of each parental AAV serotype to the evolved capsids, we performed fragment crossover mapping (Figure 3A), structural capsid mapping (Figure 3B), and predictive fragment conservation analyses (Figure S2B). These complementary methodologies demonstrated selection for certain residues and highlighted both unique and shared domains. Shuffling was achieved along the length of *Cap*, including VP1, VP2, VP3, and AAP. The parental serotypes that contributed the most to the evolved variants included AAVs 2, 3b, 1, and 6 in that order. None of the selected variants had appreciable contributions from unique AAV4, AAV5, AAV8, AAV9_hu14, bovine, or avian sequences. Our use of the AAV2 3′ UTR (Figure S4) downstream of the shuffled capsid open reading frames (ORFs) may explain why AAV2 had both high initial representation in the library and was selected for in the in vivo screen, because key regulatory elements reside within this sequence. It is also interesting to note the lack of selection for almost any unique AAV8 sequence in variants selected for their ability to transduce human as opposed to mouse hepatocytes. This supports our previous findings[4] and that of others in the field[3] that rAAV8 is a poor functional transducer of human hepatocytes in vivo and is better suited for mouse transduction studies.

Shuffled NP40, NP59, and NP84 capsid sequences (Figures 3A and S5) contained many fragments from parental serotypes with known liver tropism, likely explaining why these variants were selected for in the initial in vivo screen in humanized liver xenografts. Each of these three shuffled capsids would be predicted to have similar comparative structures to one another given their highly similar

capsid sequences (Figures 3A and 3B). NP40 is the most shuffled of the three, with the unique region of VP1 from AAV1/3b/6/8/9, the unique region of VP2 derived from AAV2, and finally VP3 with contributions from AAV2 and AAV3b, as well as one de novo mutation (K555E). As with the other variant capsids, we saw a conserved contribution from AAV3b at positions 326–426, suggesting that this is the minimal structural region from AAV3b required for enhanced human hepatic transduction. NP59 is similar to NP40 but lacks the diverse VP1 contributions and is instead composed of AAV2 in that sequence stretch. NP59 has the same VP2 and VP3 contributions as NP40 except for one de novo mutation (N622D). NP84 shares the unique regions of VP1 and VP2 with NP59, but has a much larger contribution from AAV3b and less from AAV2 in VP3, as well as two de novo mutations (K555E and R611G). Looking globally at all three variant capsids, structural mapping highlighted the subtle structural heterogeneity in hypervariable regions but also macro-conservation within key structural domains such as the cylinder (from AAV2), canyon (from AAV3b), and various symmetry axes.

Assessing Functional Hepatocyte Transduction in Xenograft Liver Models In Vivo

To rigorously assess the functional human hepatic transduction capabilities of our shuffled capsids in an appropriate in vivo setting, we transduced humanized FRG xenograft mice. To reduce bias and maximize stringency, we produced cohorts of xenografted liver mice in two different laboratories and administered variant (NP40, NP59, and NP84) or control (LK03 and DJ) rAAV capsids expressing GFP. Humanized mice at each of the two locations were administered rAAV at the same dose (2E11 vg/mouse), via the same delivery method (i.v. lateral tail vein injection), and assessed for transduction via GFP immunohistochemistry 14 days post-AAV administration (Figures 4A and 4B). Although different promoters were used, both CAG (CMV enhancer, chicken beta-actin promoter, rabbit beta-globin splice acceptor) and LSP1 have been shown to express at similar levels in hepatocytes.[27] To assess the potential impact of repopulation percentage on transduction, we transduced one cohort at high repopulation levels and the other with low repopulation levels. The independent results from two blinded laboratories demonstrated that shuffled variants NP40 and NP59 (and in the high repopulation cohort, also NP84) had significantly increased functional human hepatocyte transduction over control serotypes (Figure 4C). Although the trend for increased transduction by variants over controls held regardless of the degree of repopulation, the average transduction level varied depending on the availability of human hepatocytes and limiting rAAV virions (Figures 4D and 4E). Transduction was seen across the hepatic lobule, where gradients in metabolic activity and possibly expression and secretion of transgene products exist.

Our new shuffled variants are highly specific for transduction of human hepatocytes. When injected i.v. into non-humanized BALB-CJ mice, the shuffled variants either functionally transduced the liver very poorly or not at all (Figure S6). Another potentially promising capsid rAAV-DJ has low nAb levels[13] but had yet to be assessed for human hepatocyte transduction. To address this, we treated six FRG mice repopulated with primary human hepatocytes with AAV-DJ-CAG-GFP and measured the transduction in both mouse and human hepatocytes. Liver immunohistochemistry for human-specific fumarylacetoacetate hydrolase (FAH) and viral GFP demonstrated low levels of functional human hepatocyte transduction (<5%) in all treated mice (Figures S7A and S7B). The results from GFP RNA fluorescent in situ hybridization (FISH) followed by sequential GFP DNA FISH on treated liver sections suggested that the block to functional human transduction occurred post-uncoating (Figures S7C–S7E), as has been seen for other capsid serotypes.[21]

In addition to treating liver diseases in vivo with i.v. delivery of rAAV, ex vivo gene delivery or gene correction studies in transplantable human hepatic organoids represents a potential future therapy for some liver diseases. To establish whether our evolved liver variants could also be used ex vivo and whether they also support our in vivo data, we performed a small GFP transduction study in primary human liver organoids. In duplicate organoid transduction assessments (Figure S8), capsids NP40, NP59, LK03, and DJ all showed high functional human liver organoid transduction over rAAV2 and rAAV8 by live imaging of GFP.

Immunological Properties of Evolved Hepatotropic AAV Variants

To predict the likelihood of rAAV neutralization in patients with pre-existing and potentially cross-reacting anti-AAV capsid antibodies, we performed both seroreactivity assays and transduction neutralization assays using serum from a variety of patient groups and nonhuman primates. First, individual human serum samples from 50 healthy US adults of each gender (Table S1) were assessed for their seroreactivity to the shuffled capsid variants and control serotypes (Figure 5A; Table S2). Shuffled variants NP40, NP59, NP84, and DJ had significantly reduced seroreactivity profiles compared to rAAV8 and LK03 ($p < 0.001$–0.0001) with previously established human neutralization frequencies.[9,10,28,29] Separately assessing seroreactivity by gender (Figure S9) demonstrated a statistically significant difference in seroreactivity against the different capsids in men and women; however, sample numbers were low and must be interpreted with caution (Table S2). While both men and women showed significantly improved seroreactivity to all shuffled variants over rAAV8, only males had significant improvements compared to LK03 ($n = 33$). Female patients did not demonstrate significant seroreactivity differences between LK03 and each of the three new variant capsids (NP40, NP59, and NP84), albeit from low patient numbers ($n = 17$).

To support future pre-clinical testing in nonhuman primates, we also assessed seroreactivity with serum from a small cohort of six rhesus macaques (Table S3) against the same panel of AAVs (Figure 5B). Given the small cohort size, no statistically significant difference was seen for mean seroreactivity between the tested capsids (Table S4), with the exception that seroreactivity against AAV-DJ was significantly lower than AAV8 ($p < 0.01$). In vitro neutralization assays in human 2V6.11 permissive cells using serum from a limited cohort of 21 healthy human donors from the European Union (E.U.) found mean similarity across all serotypes (Figure 5C; Table S5). Although

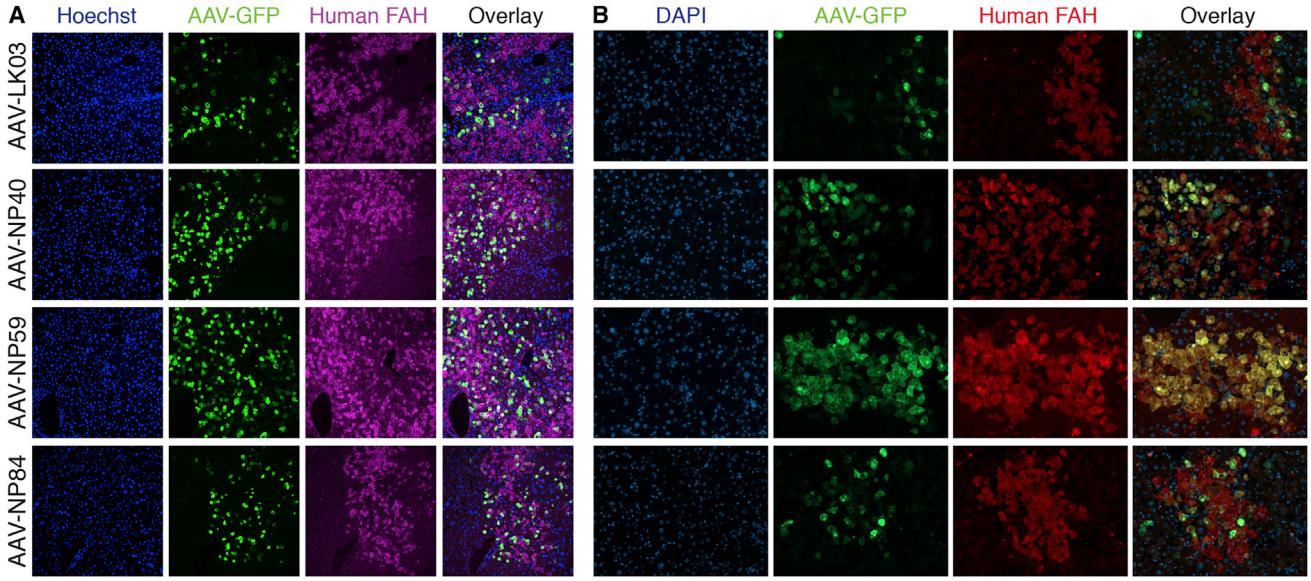

C

Serotype	Transfer vector	# of FRG	Gender of FRG recips	hAlb/mouse (mg/ml)	# of Fah+ human heps counted	# of GFP+ human heps	Average GFP+ human heps	Location
NP40	ssAAV-LSP1-GFP	2	2F	4.95, 0.73	2,244	1,673	72.8%	CMRI
NP59	ssAAV-LSP1-GFP	3	1M, 2F	0.25, 0.36, 0.29	2,563	2,450	94.5%	CMRI
NP84	ssAAV-LSP1-GFP	3	1M, 2F	0.04, 0.23, 0.38	988	219	27.7%	CMRI
LK03	ssAAV-LSP1-GFP	2	2F	0.06, 0.13	592	178	32.6%	CMRI
NP40	ssAAV-CAG-GFP	1	1M	8.01	2,175	688	31.6%	OHSU
NP59	ssAAV-CAG-GFP	1	1M	4.65	1,831	661	36.1%	OHSU
NP84	ssAAV-CAG-GFP	1	1F	3.91	1,404	424	30.2%	OHSU
LK03	ssAAV-CAG-GFP	1	1F	3.87	2,276	380	16.7%	OHSU

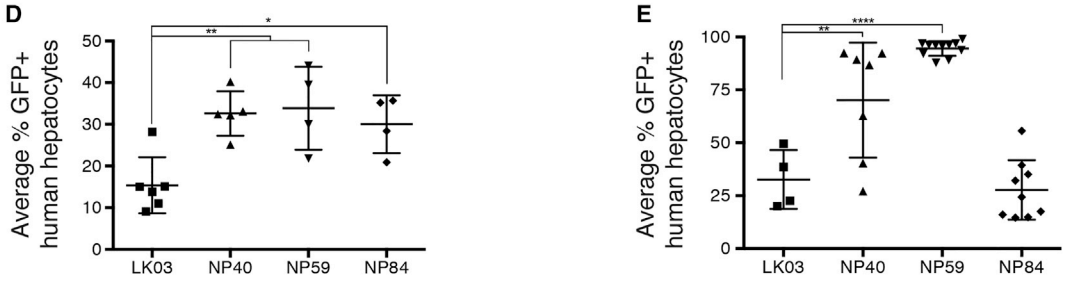

Figure 4. Validation and Comparative Quantitation of Human Hepatocyte Transduction in Humanized Liver Mice In Vivo

(A) Representative immunohistochemical images from treated humanized liver mice from Oregon Health & Science University (OHSU) transduced with ssAAV-CAG-GFP at 2E11 vg i.v. with varying capsid serotypes. Human-specific FAH (violet), viral-GFP (green), and Hoechst (blue) on liver cross sections. 20× magnification. (B) Representative immunohistochemical images from treated humanized liver mice from Children's Medical Research Institute (CMRI) transduced with ssAAV-LSP1-GFP at 2E11 vg i.v. with varying capsid serotypes. Human-specific FAH (red), viral-GFP (green), and DAPI (blue) on liver cross sections. 20× magnification. (C) Summary of analysis from transduced xenografted FRG mice at each location. (D) Comparative mean ± SD transduced human hepatocytes per slide in the high repopulation cohort from OHSU. *$p < 0.05$; **$p < 0.01$. (E) Comparative mean ± SD transduced human hepatocytes per slide analyzed in the low repopulation cohort from CMRI. **$p < 0.01$; ****$p < 0.0001$. F, female; hAlb, human albumin; M, male.

all shuffled variants had lower mean levels of neutralization than LK03, only rAAV8 reached statistical significance ($p < 0.001$) in this small cohort ($n = 21$). One important potential application of these capsids relates to hemophilia B trials. Thus, we also performed seroreactivity assays with serum from 21 adult males with hemophilia B (Table S6). Due to sample limitations, we compared the variants to only the leading candidate, LK03. Results showed that compared to LK03, NP59 had more favorable mean seroreactivity in 66% of patients, whereas both NP84 and NP40 were more favorable in 53% of patients, although they did not reach statistical significance in this small cohort (Figure 5D; Table S6). In vitro neutralization assays in human 2V6.11 permissive cells using pooled human immunoglobulins from thousands of human donors demonstrated that NP40, NP59, and NP84 have neutralization similar to AAV-DJ and AAV8, but unlike AAV-LK03 and AAV3b (Figure 5E). Cumulatively, these findings highlight the unique immunological features of variant capsids particularly when it comes to seroprevalence and antibody-mediated neutralization. More globally, patients with high nAb titers

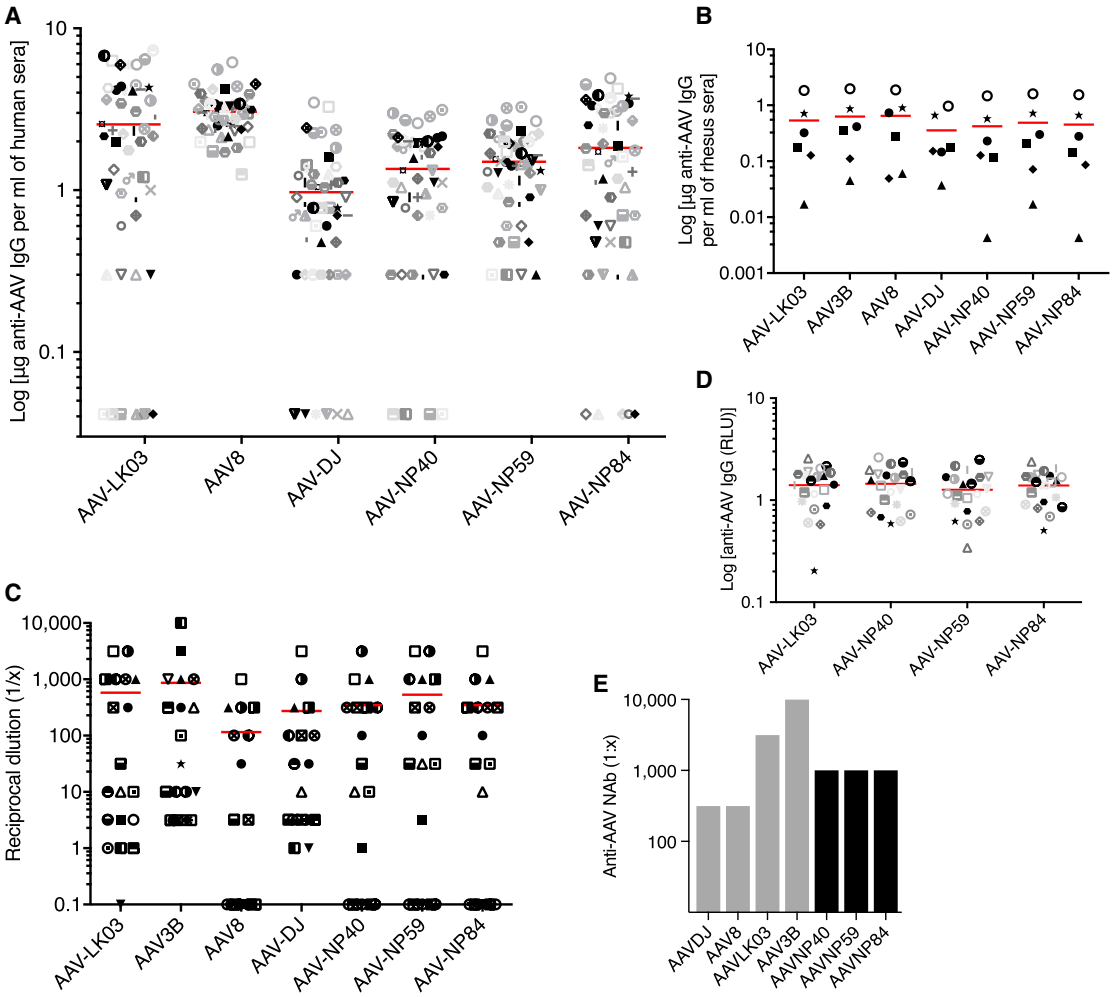

Figure 5. Immunological Assays across Key Patient Groups and Nonhuman Primates

(A) Seroreactivity ELISA assay for presence of anti-AAV antibodies in normal human serum from 50 US adults. Each patient was assayed in technical triplicates with data points representing the mean minus background. Red line represents the mean. Symbols are consistent across treatments for each patient to allow comparisons. (B) Seroreactivity ELISA assay for the presence of anti-AAV antibodies in serum from six rhesus macaques. Each dot is one macaque. Red line represents the mean. (C) Human 2V6.11 AAV-permissive cells were used to assess rAAV neutralization in the presence of patient serums for 21 E.U. individuals. Data show the reciprocal dilution at which >50% inhibition of transduction was observed. Red line represents the mean. (D) Seroreactivity ELISA assay for the presence of anti-AAV antibodies in human serum from 21 adult males with hemophilia B. Red line represents the mean. (E) Human 2V6.11 AAV-permissive cells were used to assess rAAV neutralization in the presence of pooled human immunoglobulins (Octagam IVIG) from thousands of patients. Data show the reciprocal dilution at which >50% inhibition of transduction was observed.

against any one serotype did not necessarily correlate with high nAb titers against other serotypes, suggesting that sera from individual patients needs to be assessed against a broad panel of capsid serotypes.

DISCUSSION

Choosing the best rAAV serotype for optimum human hepatic delivery has grown increasingly complex and controversial in recent years stemming from differences in experimental setup, data interpretation, and reproducibility.[3,4,30,31] Given the number of altered variables in experimental design by different groups, this is perhaps not surprising. No two studies have been performed identically; thus, comparisons have and will continue to be confounded. At its simplest, use of different model systems for assessment has created difficulties. It is well-known that rAAV transduction in in vitro culture systems does not correlate with in vivo transduction levels; thus, testing in these lines for the strict purpose of establishing functional in vivo transduction without any other supportive data should be abandoned. Even with in vivo transduction measurements, use of different species with no human xenograft (mice) has been shown not to recapitulate transduction outcomes in humans,[1,5] and such results should be interpreted with caution. Although no model organism perfectly recapitulates a human liver, current evidence demonstrates that assessing functional transduction in xenograft liver models engrafted with primary human hepatocytes has best recapitulated existing patient data

to date.[3,4] Similarly, quantifying functional transduction by vector copy number (VCN) is inaccurate because it measures all genomes post-entry irrespective of functionality. This is critically important quantitatively because most AAV genomes do not complete the intracellular trafficking and expression cascade[32,33] required for therapeutic relevance; thus, extrapolating functional transduction from VCN measurements is misleading and can lead to gross overestimations.

Replicating AAV screens present both opportunities and challenges. Although they have great potential to select for the most relevant variants capable of all steps in functional transduction, caution must be applied when executing them. First, the human adenoviruses needed to replicate the AAV library require human cells for replication, and not all human cell types support adenoviral uptake and replication. Second, screening in human xenografts in vivo is challenging because mouse hepatocytes remain, and controlling the percent human repopulation is difficult. Third, careful monitoring via sequencing and functional assays is needed to ensure that variants are selecting on the applied selective pressure and not merely for those variants that best replicate in that cell type.

In this study, we demonstrated the potential importance of controlling for and reporting the repopulation levels in humanized mice because the relative ratio of mouse to human hepatocytes was likely critical to overall transduction efficiency levels when rAAV virions were limiting. Further studies directly addressing these phenomena at length are needed. To date, it has been challenging to even attempt to reproduce studies published in the field because of the lack of providing detailed methods and low numbers of treated subjects in animal studies. Moving forward, to facilitate comparisons between future studies, additional variables should also be stringently controlled and reported, including detailed mouse maintenance conditions, strain backgrounds of mice or other animal models, human hepatocyte donor characteristics (age, gender, disease state, location), method of injection, AAV production and purification methods employed, detailed transfer vector descriptions (including promoter, transgene, enhancer, polyA, genome type, etc.), method of titration, final resuspension solution, method of quantifying vector transduction, and any normalizations performed.

High levels of pre-existing nAbs against parental serotypes in patients treated to date have made pre-screening a requirement for all future trials. Prevalence of nAbs varies with patient geography, health status, gender, age, and likely many other variables.[34] Therefore, panels of vetted capsids with varying parentage and different neutralization potentials are needed to enable future liver gene therapy trials with maximum patient enrolment. Among known hepatotropic serotypes, the limited human studies to date have shown highest nAb levels against rAAV2,[9,10,28,29,35] rAAV5,[10,29,35,36] rAAV8,[10,28,29] and rAAV3b.[9,29] However, the field needs a more robust methodology to assess human neutralization potential because many existing methods are difficult to perform and interpret, particularly for those serotypes that naturally transduce poorly in vitro. Further, few antigenic epitopes have been characterized for parental serotypes or shuffled variants, thus precluding rational design attempts that still maximize capsid library diversity. Vetting future capsid variants in preclinical validations against pools of patient antibodies across many patient demographics represents an unbiased approach to improve the ultimate utility of variants moving into the clinic.

An exciting possibility with our new capsid variants that transduce human liver at such high levels would be to decrease patient doses while still enabling desired expression levels. This could bypass several remaining hurdles to rAAV being an effective vector for future liver gene therapy trials: (1) reduced production costs to offset the staggering treatment costs that can reach $1 million dollars per patient;[37,38] and (2) reduced probability for capsid-specific T cell responses against transduced hepatocytes.[39] Similarly, high-level functional transduction will be key for the field as we collectively transition from treating simple non-cell-autonomous liver diseases like Crigler-Najjar and the hemophilias to cell-autonomous diseases like ornithine transcarbamylase deficiency and other urea cycle disorders, which will require at least 20%–50% of human hepatocytes to be functionally transduced for clinical efficacy.

MATERIALS AND METHODS

Shuffled AAV Capsid Plasmid Library Generation

The shuffled AAV capsid library was generated as described previously[4] with modifications described below. The AAV capsid genes from serotypes 1, 2, 3b, 4, 5, 6, 8, 9_hu14, avian, and bovine were PCR-amplified with high-fidelity polymerase and cloned using a Zero Blunt TOPO PCR Cloning Kit (catalog [Cat] no. K2800; Invitrogen) followed by Sanger sequencing of individual clones. Capsid genes were excised, mixed at 1:1 ratios, and digested using DNase I at various intervals from 1 to 30 min. These pooled reactions were separated on a 1% (w/v) agarose gel, and fragments <1,000 bp were excised and used in a primer-less PCR reassembly step, followed by a second round of PCR using primers binding outside the capsid gene: forward (Fwd): 5′-GTCTGAGTGACTAGCATTCG-3′; reverse (Rev): 5′-GCTTACTGAAGCTCACTGAG-3′.

Full-length shuffled capsid genes were cloned into a modified pAAV2 host plasmid (inverted terminal repeat [ITR]-*Rep*2-*Cap* cloning site-AAV2 3′ UTR sequence-ITR) with SwaI/NsiI restriction sites flanking the CAP insertion site and a modified portion of the AAV2 VP1 3′ UTR (Figure S4). Ligations were transformed into numerous independent electro-competent cell aliquots and diluted 1:40 in Luria broth (LB) culture with low ampicillin (50 g/mL) for minimal expansion. An aliquot was plated, and 100 clones were picked and Sanger sequenced to validate library diversity. The pool of library plasmids was purified using an EndoFree Plasmid Mega Kit (Cat. no. 123811; QIAGEN) and used to produce libraries of replication-competent AAV virions.

AAV Library Production, Vector Production, and Titration

AAV library productions were produced using a $Ca_3(PO_4)_2$ transfection protocol (WT AAV library plasmid pool and pAd5 helper) in HEK293T cells (Cat. no CRL-3216; ATCC) followed by double

cesium chloride density gradient purification, dialysis as previously described,[40] and resuspension in Dulbecco's PBS (dPBS) with 5% sorbitol (w/v) and 0.001% Pluronic F-68 (v/v). AAV libraries were titered for *Rep* by TaqMan qPCR with the following primer/probe set: Fwd: 5′-TTCGATCAACTACGCAGACAG-3′; Rev: 5′-GTCCGTGAGT GAAGCAGATATT-3′; Probe: 5′/FAM/TCTGATGCTGTTTCCC TGCAGACA/BHQ-1/-3′.

rAAV vector productions were similarly produced as above but as triple transfections (polyethylenimine [PEI] or $Ca_3(PO_4)_2$) with pAd5 helper, AAV transfer vector (single-stranded AAV [ssAAV]-CAG-GFP-WPRE-SV40pA from Addgene 37825; ssAAV-EF1a-FLuc-WPRE-HgHpA from Addgene 87951; ssAAV-LSP1-GFP-WPRE-BgHpA from Ian Alexander[41]), and pseudotyping plasmids for each capsid of interest. AAV-GFP vectors were titered on GFP by TaqMan qPCR with the following primer/probe set: Fwd: 5′-GACGTAAACG GCCACAAGTT-3′; Rev: 5′-GAACTTCAGGGTCAGCTTGC-3′; Probe: 5′/FAM/CGAGGGCGATGCCACCTACG/BHQ-1/-3′. AAV-FLuc vectors were titered by TaqMan qPCR with the following primer/probe set: Fwd: 5′-CACATATCGAGGTGGACATTAC-3′; Rev: 5′-TGGTTTGTATTCAGCCCATAG-3′; Probe: 5′/FAM/ACT TCGAGATGAGCGTTCGGCTG/BHQ-1/-3′.

Mice

Fah/Rag2/Il2rgc-deficient mice[25] on a C57BL/6J background and FRG mice on an non-obese diabetic (NOD) strain background (FRG/N) were housed and maintained in specific pathogen-free barrier facilities at either Oregon Health & Science University (US), Stanford University (US), or the Children's Medical Research Institute (Australia). FRG/N mice were maintained on irradiated high-fat, low-protein mouse chow (US: Lab Diet Cat. no. Picolab-5LJ5; Australia: Specialty Feeds Cat. no. S415-024) ad libitum to decrease flux through the tyrosine pathway. Beginning on the day of transplantation, FRG/N mice in the US were maintained on 1 week of acidified water to prevent bacterial growth, whereas mice in Australia received acidified water supplemented with 25 mg/mL Baytril antibiotic. The following week, mice in the US were switched to 1 week of 8 mg/L sulfamethoxazole-trimethoprim (SMX-TMP) antibiotic water (supplemented with 0.7 mol/L dextrose for palatability), whereas mice in Australia were switched to 1 mg/L 2-(2-nitro-4-trifluoromethylbenzoyl)-1,3-cyclohexanedione (NTBC) water. Thereafter, at each location, FRG/N mice were cycled on and off 1 mg/L NTBC water as described.[25,42] Adult Balb/cJ mice were purchased from The Jackson Laboratories (Cat. no 00651) for imaging studies. The Institutional Animal Care & Use Committees of Stanford University, Oregon Health & Science University, and the Children's Medical Research Institute approved all mouse procedures.

Hepatocyte Transplantation

Donor human hepatocytes for transduction studies were acquired from either Celsis (Cat. no F00995; Lot no. LTS) from a 17-year-old white female for US studies or from Lonza (Cat. no. CC-2591S, Lot no. 9F3097) from a white male for Australian studies. Weanling FRG/N mice were pre-conditioned with administration of recombinant human adenovirus expressing urokinase (1.25E9 plaque-forming units (PFUs) by tail vein in Australia and 5E10 PFUs retroorbitally in USA) 24 hr prior to transplant to promote human cell engraftment. 5E5–1E6 human hepatocytes were injected intrasplenically into anesthetized recipient FRG/N mice and cycled on/off NTBC to promote human hepatocyte engraftment and expansion.[25] Broad-spectrum antibiotic (ceftiofur 4 mg/kg in US; Baytril 5.6 mg/kg in Australia) was given by intraperitoneal injection immediately prior to surgery and for 2 days following surgery. Several weeks post-transplant, circulating human albumin levels were used to assess percent human engraftment from several microliters of peripheral mouse blood.

Human Albumin ELISA

To assess percent human engraftment in chimeric mice, we used several microliters of peripheral blood to measure human albumin using the Bethyl Quantitative Human Albumin ELISA kit (Cat. no E88-129) per manufacturer's protocol. This same kit was used to detect secreted human albumin levels in the media supernatant during human hepatic organoid differentiation as a marker of successful differentiation.

Replication-Competent AAV Library Selection in Humanized FRG Mice

Female FRG mice with confirmed humanization, and maintained on 1 mg/L NTBC, were transduced with 5E10 vg/mouse of AAV library by i.v. tail vein administration. 5E9 PFUs of wild-type replication-competent human Adenovirus-5 (hAd5) (Cat. no. VR-5; ATCC) in 20 μL volume was administered by i.v. retroorbital injection 24 hr later. Transduced humanized livers were harvested 48 hr after hAd5 administration. Livers were minced, subjected to three freeze-thaw cycles, and further homogenized to ensure complete lysis of remaining hepatocytes. Liver lysates were then subjected to 65°C for 30 min to heat-inactivate the hAd5 and spun at 14,000 revolutions per minute (RPM) at 4°C to separate viral-containing supernatants from cellular debris. Viral supernatants were dot-blot titered after each round to ensure continual administration of 5E10 vg/mouse at each subsequent round of in vivo selection for a total of five rounds.

Sequential Subscreen on Evolved Human Liver Library against Pooled Human Immunoglobulins

PureProteome protein G magnetic beads (Cat. no. LSKMAGG02; Millipore) were pre-loaded with pooled human immunoglobulins (Baxter Gammagard IVIG Liquid; Cat. no. LE1500190, Lot no. LE12J338AB) for 60 min at 4°C per bead manufacturer's instructions for direct immunoprecipitation protocols. The AAV library from round 5 of the in vivo screen was applied to the IgG-loaded beads for 12 hr rotating at 4°C. Bound and unbound fractions were natively eluted per manufacturer's instructions and run over a new set of IgG-loaded beads to enrich for true IgG-bound and unbound AAV populations. Viral genomic DNA (gDNA) was extracted from each fraction using the MinElute Virus Spin Kit (Cat. no. 57704; QIAGEN), followed by PCR amplification

using: Fwd: 5′-TGGATGACTGCATCTTTGAA-3′; Rev: 5′-TGCTTACCCGGGTTACGAGTCAGGTATCTG-3′.

AAV capsid ORFs from round 2 of the subscreen for IgG evasion were cloned using a Zero Blunt TOPO Kit, and 100 clones were sent for full Sanger sequencing to assess diversity with primers: Fwd-1: 5′-TGGATGACTGCATCTTTGAA-3′; Fwd-2: 5′-ATTGGCATTGCGATTCC-3′; Rev-1: 5′-ATGGAAACTAGATAAGAAAGAA-3′.

Vectorization and Sequence Contribution Analysis of Evolved AAV Capsids

Contigs were assembled using Geneious R7 v7.1.9 software, and clones selected for vectorization were amplified using: Fwd: 5′-AAATCAGGTATGGCTGCCGATG-3′; Rev: 5′-GCTTCCCGGGATGGAAACTAGATAAGAAAG-3′. PCR amplicons were cloned in-frame, downstream of *Rep*, into predigested recipient pCap packaging plasmid containing AAV2 *Rep* without ITRs using SwaI and XmaI restriction sites. AAV capsid genes were sequence verified, and resultant contigs were analyzed using a custom Perl pipeline that assesses multiple sequence alignments using Clustal Omega (EMBL-EBI) to generate the overall serotype composition of the shuffled AAVs by comparison of DNA and amino acid sequences with the parental AAV serotypes based on maximum likelihood. Xover 3.0 DNA/protein shuffling pattern analysis software was used to generate parental fragment crossover maps of shuffled variants.[43] Each parental serotype was color-coded as follows: AAV1: red; AAV2: forest green; AAV3b: marine blue; AAV4: magenta; AAV5: tv blue; AAV6: green cyan; AAV8: orange; AAV9: pale green; avian: purple; bovine: deep salmon.

PacBio Library Preparation and Full-Length Single-Molecule Capsid Sequencing

PacBio SMRT bell libraries were prepared following the "Procedure and Checklist-2 kb Template Preparation and Sequencing" protocol from PacBio using the SMRTbell Template Prep Kit v1.0 (Cat. no. 100-259-100; PacBio). PacBio "Binding and Annealing" calculator was used to determine appropriate concentrations for annealing and binding of SMRTbell libraries. SMRTbell libraries were annealed and bound to P6 DNA polymerase for sequencing using the DNA/Polymerase Binding Kit P6 v2.0 (Cat. no 100-372-700; PacBio). Bound SMRTbell libraries were loaded onto SMRT cells using standard MagBead protocols and the MagBead Buffer Kit v2.0 (Cat. no. 100-642-800; PacBio). The standard MagBead sequencing protocol was followed with the DNA Sequencing Kit 4.0 v2 (Cat. no. 100-612-400, also known as P6/C4 chemistry; PacBio). Sequencing data were collected for 6 hr movie times with "Stage Start" not enabled. Circular consensus sequence (CCS) reads were generated using the PacBio SMRT portal and the RS_ReadsOfInsert.1 protocol, with filtering set at Minimum Full Pass = 3 and Minimum Predicted Accuracy = 95%.

Bioinformatics Assessment of PacBio Sequence Reads

CCS reads with full capsid sequence lengths from 2,300 to 2,350 nt were included in downstream bioinformatics analyses. Indels in CCS reads were corrected using an in-house algorithm that first assesses parental fragment identity using Xover 3.0 DNA/protein shuffling pattern analysis software.[43] Once the parental identity of each crossover fragment was determined, this information was used to determine indels for correction. SNPs that did not result in indels were maintained. The SNP error rate with the PacBio platform is 1.3%–1.7%.[44,45] SNP frequencies above this rate range were assumed to have arisen from de novo mutations. Corrected sequences in FASTA format were then aligned with MUSCLE.[46] Phylogenetic analyses were conducted using the maximum-likelihood method in RAxML.[47] Percent parental conservation was determined using an in-house algorithm that identifies the percentage of each parent on each aligned position in the shuffled library. The maximum square size indicates that 100% of variants share that amino acid from that parent at that position. All other square sizes are proportional to the percent of variants from 0%–100% that have that amino acid at that position from that parent.

Transduction Mouse Experiments

All mice received normodynamic i.v. lateral tail vein injections of 2E11 vg/mouse ssAAV-CAG-GFP or ssAAV-LSP1-GFP pseudotyped with various capsid serotypes. Treated mice were monitored for 14 days (humanized FRG mice were maintained on 1 mg/L NTBC during this 14-day transduction), and livers were harvested under inhalation isoflurane anesthesia. Liver tissue was cut into several 2 × 5-mm pieces from several lobes and fixed in 10× volume of 4% paraformaldehyde (PFA) for 5 hr at 25°C protected from light. Fixed tissue was washed 1× in PBS and put through a sucrose cryoprotection and rehydration series (10% w/v sucrose for 2 hr at 25°C, 20% w/v sucrose overnight at 4°C, 30% w/v sucrose for 4 hr at 25°C). Liver pieces were rinsed in PBS, blotted dry, mounted in cryomolds (Cat. no. 4557; Tissue-Tek) with optimal cutting temperature (OCT) (Cat. no. 4583; Tissue-Tek), and frozen in a liquid nitrogen-cooled isopentane bath. Labeled cryomolds were wrapped in aluminum foil and placed at −80°C until sectioning.

Liver Immunohistochemistry

Fluorescent staining of liver sections for human FAH was performed per established protocols[48] with minor modifications. Modifications included fixing slides in ice-cold methanol for 10 min rather than acetone at room temperature; blocking with 10% rather than 5% donkey serum (Cat. no. sc-2044; Santa Cruz) in dPBS for 30 min at room temperature (RT) in a humidified chamber; primary antibody solution was 100 µL of monoclonal rabbit anti-human FAH IgG antibody (Cat. no. HPA-04137; Sigma) at 1:100 (Australia) or 1:500 (US) in 10% donkey serum incubated overnight at 4°C (US) or for 2 hr at RT (Australia); secondary antibody solution was 100 µL of donkey anti-rabbit Alexa Fluor 647 IgG antibody (Cat. no. A31573; Invitrogen) at 1:500 along with Hoechst 33342 (Cat. no. H-3570; Molecular Probes) at 1:1,000 in PBS with tween (PBST) for 1 hr at RT in dark conditions (US), or 100 µL of donkey anti-rabbit Alexa Fluor 594 IgG antibody (Cat. no. A21207; Invitrogen) at 1:500 in PBS for 1 hr at RT in dark conditions followed by DAPI at 80 ng/mL in PBS; and slides were mounted with 3 drops of ProLong

Gold Antifade (Cat. no. P36934; Invitrogen) (US) or ProLong Diamond Antifade (Cat. no. P36961; Invitrogen) (Australia). Antibody validity controls included secondary-only staining and demonstration on positive control frozen human liver tissue sections (Cat. no. HF-314; Zyagen) and negative control frozen untreated mouse liver sections. Confocal imaging in the USA was performed on a Leica TCS SP8-X WLL inverted confocal microscope with a 20× oil immersion objective and imaged with Leica AF software v3.3.0.10134, whereas confocal imaging in Australia was performed on an inverted Zeiss Axio with 20× objective and imaged with Zen Pro software. Z stacks were compressed using ImageJ v2.0.0 and overlaid in Adobe Photoshop CS6 v13.0. Signal co-localization of AAV-GFP signal with mouse or human hepatocytes was done using Volocity v6.3 software and re-validated with counts by eye on a subset of sections.

Hepatic FISH

Sequential RNA and DNA FISH on OCT-embedded frozen liver sections from treated humanized mice was performed as described.[49] To localize RNA FISH signals, we analyzed slides by acquiring multiple 3D images, recording coordinates of all imaged fields, and combining planes from each field using an EDF (extended depth of focus) function into a series of single-focused images for each imaged field. Subsequent DNA FISH was completed as described,[49] and the previously imaged fields were imaged again in the same manner. Comparing the image sets allows one to determine the relative position of RNA and DNA signals. The addition of GFP immunostaining showed the relationship between transcription and translation of AAV transfer vector DNA. Images were taken on a Nikon Eclipse E800 wide-field microscope (60X Plan Apochromat objective with 1.4-NA) with a Photometrics Coolsnap ES camera and Nikon NIS Elements software v4.2.

Functional Validation of Human Hepatic Organoid Cultures

Human liver non-parenchymal cells from a 23-year-old male were cultured as described[50,51] with minor modifications (gastrin was omitted and ALK5 inhibitor SB431542 was added). To functionally demonstrate hepatic origin of organoids, we tested media from organoid cultures for the presence of human albumin by ELISA (human albumin = 58.3 ng/mL).

Human Hepatic Organoid Transduction with AAV

Initiated hepatic organoid cultures were passaged at a ratio of 1:4 into standard organoid conditions (embedding in >95% Matrigel followed by addition of liquid media) in 24-well suspension plates after 2 weeks of growth. After the fifth organoid passage, ssAAV-CAG-GFP preparations of each serotype were added at MOI 500K to each well. Media were changed after a 3-day incubation and daily thereafter, and the emergence of GFP expression was monitored daily by fluorescence microscopy and bright-field imaging. Maximum expression was reached at approximately day 11, and that is when images were taken.

Indirect Seroreactivity ELISA Assay for Anti-AAV Antibodies in Human Serum

Off-clot serum collected from peripheral blood of 50 healthy US adults (Table S1) was used as the primary antibody in an indirect ELISA. Pooled human IgG (Cat no. LE1500190, Lot no. LE12P180AB; Baxter) from thousands of donors was used to prepare a standard curve (sixteen 2-fold dilutions of 100 mg/mL stock i.v. immunoglobulin [IVIG] in blocking buffer). Shuffled and parental AAV capsids served as antigens (5E8 vg/well). Human IgG standards were assessed in replicates of six, and all AAV samples were assessed in triplicate. IgG standards and AAV samples were fixed to wells of a 96-well immunoplate with 50 µL of coating solution (13 mM Na_2CO_3, 35 mM $NaHCO_3$ in water [pH 9.6]); plates were sealed and incubated overnight at 4°C. Plates were washed 2× with PBST containing 0.05% Tween 20 and blocked with blocking buffer (PBS, 6% BSA, 0.05% Tween 20) for 1 hr at 25°C. Plates were washed 2× with PBST. Each of the 50 human sera samples was diluted in blocking buffer (1:100–2,000), and 50 µL was added to experimental wells. Plates were incubated for 2 hr at 37°C and then washed 2× in PBST. Polyclonal sheep anti-human IgG-HRP secondary antibody (Cat. no. NA933V; GE Bioscience) was diluted 1:500 in wash buffer and 100 µL was added to each well to detect bound antibodies in the human sera. Plates were incubated for 2 hr at 37°C and washed 2× in PBST. OPD substrate (o-phenylenediamine dihydrochloride; Cat. no. P4664; Sigma) was added at 100 µL/well in a 0.1 M sodium citrate buffer, and plates were incubated at 25°C for exactly 10 min. The reaction was stopped with 50 µL/well of 3 M H_2SO_4, and the absorbance was determined at 490 nm on a microplate reader (Bio-Rad). A set of blank wells was used to subtract background for non-specific binding of antibodies to the immunoplate. Standards were plotted using four-parameter logistic curve fitting to determine sample concentrations that fall within the linear range of the dilution series and detection limits using Prism v6.0 software. The same assay was performed on a cohort of 21 adult males with hemophilia B (Table S6).

Indirect Seroreactivity ELISA Assay for Anti-AAV Antibodies in Normal Rhesus Macaque Serum

The seroreactivity ELISA was performed as previously described[52] with plates coated at 1E9 viral proteins (vp)/well. Off-clot serum was collected from peripheral blood from six rhesus macaques (Table S3).

Luminescence-Based AAV Neutralization Assays with Individual Human Serum Samples

The neutralization assays were performed as previously described.[53] For individual patients in Figure 5C, off-clot serum was collected from peripheral blood of 21 healthy E.U. individuals (Table S5), while Figure 5E utilized pooled human immunoglobulins (Octagam IVIG) from thousands of patients. ssAAV-CMV-FLuc vector was used as the transfer vector at an MOI of 200.

False-Colored Structural Capsid Mapping

Chimeric capsids were false-color-mapped onto the AAV2 capsid structure 1LP3[54] using Pymol v1.7.6.0. Mapped colors correspond to parental serotype colors used in the parental fragment crossover maps. Exterior capsid views have all chains represented, whereas cross-sectional views have chains surrounding a cylinder at the 5-fold symmetry axis removed exposing the capsid interior lumen.

Statistics

Statistical analyses were conducted with Prism v7 and Excel v15.36 software. Experimental values for each panel in Figure 5 were log+1 transformed before being assessed via two-way ANOVA using Tukey's multiple comparisons test. The p values <0.05 were considered statistically significant. Additional experimental differences were evaluated using a Student's unpaired two-tailed t test assuming equal variance.

SUPPLEMENTAL INFORMATION

Supplemental Information includes nine figures and six tables and can be found with this article online at https://doi.org/10.1016/j.ymthe.2017.09.021.

AUTHOR CONTRIBUTIONS

N.K.P., C.L., A.P.D., L.L., M.B.V., F.M., A.M.D., A.C.N., I.A.E., M.G., and M.A.K. designed the experiments. N.K.P., K.P., E.Z., S.N., B.L., C.L., J.X., A.P.D., F.Z., L.L., K.C., A.H., Y.Z., C.M., M.B.V., and M.A.K. generated reagents, developed protocols, performed experiments, and analyzed data. N.K.P. wrote the manuscript and generated the figures. All authors reviewed, edited, and commented on the manuscript.

CONFLICTS OF INTEREST

N.K.P., L.L., and M.A.K. are inventors on patents for AAV serotypes used in this paper. F.M., A.M.D., A.C.N., and M.A.K. have patents related to AAV-mediated liver gene transfer. M.G. has patents on the FRG/N mice. F.M. and L.L. have corporate funding. A.P.D., M.G., L.L., A.C.N., I.A.E., and M.A.K. have commercial affiliations. N.K.P., E.Z., F.M., L.L., M.G., I.A.E., and M.A.K. have consulted on technologies broadly related to this paper. M.G., L.L., and M.A.K. have stock and/or equity in companies with technology broadly related to this paper. All other authors declare no conflicts of interest.

ACKNOWLEDGMENTS

The authors wish to acknowledge Derek Pouchnik and Mark Wildung of the WSU Laboratory for Biotechnology & Analysis for sequencing help. N.K.P. was supported by postdoctoral fellowships from the National Heart Lung & Blood Institute (grant F32-HL119059), the American Liver Foundation Hans Popper Memorial Fellowship, and the Stanford Dean's Fellowship. This work was supported by grants to M.A.K. from the NIH (grant R01-HL092096); to M.V. from the NIH (grant P30-CA21765); to A.D. from the NIH (grant R01-HL073838), the ALSAC St. Jude Children's Research Hospital, and the Assisi Foundation of Memphis; to M.G. from the NIH (grant R01-DK048252); to F.M. from the ERC (grant CoG-617432); and to I.E.A. from the Australian NHMRC (grant APP-1008021). This project was supported by a NIH Shared Instrumentation Grant (S10-OD01058001-A1) from the NCRR with significant contribution from Stanford's Beckman Center, as well as the OHSU Flow Cytometry Shared Resource. The contents of this publication are solely the responsibility of the authors and do not necessarily represent the official views of the various funding bodies or universities involved. Packaging plasmids for any of the new capsids described herein must be obtained through a material transfer agreement (MTA) with Stanford University.

REFERENCES

1. Nathwani, A.C., Reiss, U.M., Tuddenham, E.G., Rosales, C., Chowdary, P., McIntosh, J., Della Peruta, M., Lheriteau, E., Patel, N., Raj, D., et al. (2014). Long-term safety and efficacy of factor IX gene therapy in hemophilia B. N. Engl. J. Med. *371*, 1994–2004.

2. Manno, C.S., Pierce, G.F., Arruda, V.R., Glader, B., Ragni, M., Rasko, J.J., Ozelo, M.C., Hoots, K., Blatt, P., Konkle, B., et al. (2006). Successful transduction of liver in hemophilia by AAV-Factor IX and limitations imposed by the host immune response. Nat. Med. *12*, 342–347.

3. Vercauteren, K., Hoffman, B.E., Zolotukhin, I., Keeler, G.D., Xiao, J.W., Basner-Tschakarjan, E., High, K.A., Ertl, H.C., Rice, C.M., Srivastava, A., et al. (2016). Superior in vivo transduction of human hepatocytes using engineered AAV3 capsid. Mol. Ther. *24*, 1042–1049.

4. Lisowski, L., Dane, A.P., Chu, K., Zhang, Y., Cunningham, S.C., Wilson, E.M., Nygaard, S., Grompe, M., Alexander, I.E., and Kay, M.A. (2014). Selection and evaluation of clinically relevant AAV variants in a xenograft liver model. Nature *506*, 382–386.

5. Nathwani, A.C., Tuddenham, E.G., Rangarajan, S., Rosales, C., McIntosh, J., Linch, D.C., Chowdary, P., Riddell, A., Pie, A.J., Harrington, C., et al. (2011). Adenovirus-associated virus vector-mediated gene transfer in hemophilia B. N. Engl. J. Med. *365*, 2357–2365.

6. Li, C., Narkbunnam, N., Samulski, R.J., Asokan, A., Hu, G., Jacobson, L.J., Manco-Johnson, M.J., and Monahan, P.E.; Joint Outcome Study Investigators (2012). Neutralizing antibodies against adeno-associated virus examined prospectively in pediatric patients with hemophilia. Gene Ther. *19*, 288–294.

7. Erles, K., Sebökovà, P., and Schlehofer, J.R. (1999). Update on the prevalence of serum antibodies (IgG and IgM) to adeno-associated virus (AAV). J. Med. Virol. *59*, 406–411.

8. Calcedo, R., Morizono, H., Wang, L., McCarter, R., He, J., Jones, D., Batshaw, M.L., and Wilson, J.M. (2011). Adeno-associated virus antibody profiles in newborns, children, and adolescents. Clin. Vaccine Immunol. *18*, 1586–1588.

9. Ling, C., Wang, Y., Feng, Y.L., Zhang, Y.N., Li, J., Hu, X.R., Wang, L.N., Zhong, M.F., Zhai, X.F., Zolotukhin, I., et al. (2015). Prevalence of neutralizing antibodies against liver-tropic adeno-associated virus serotype vectors in 100 healthy Chinese and its potential relation to body constitutions. J. Integr. Med. *13*, 341–346.

10. Liu, Q., Huang, W., Zhang, H., Wang, Y., Zhao, J., Song, A., Xie, H., Zhao, C., Gao, D., and Wang, Y. (2014). Neutralizing antibodies against AAV2, AAV5 and AAV8 in healthy and HIV-1-infected subjects in China: implications for gene therapy using AAV vectors. Gene Ther. *21*, 732–738.

11. Liu, Q., Huang, W., Zhao, C., Zhang, L., Meng, S., Gao, D., and Wang, Y. (2013). The prevalence of neutralizing antibodies against AAV serotype 1 in healthy subjects in China: implications for gene therapy and vaccines using AAV1 vector. J. Med. Virol. *85*, 1550–1556.

12. Mingozzi, F., Maus, M.V., Hui, D.J., Sabatino, D.E., Murphy, S.L., Rasko, J.E., Ragni, M.V., Manno, C.S., Sommer, J., Jiang, H., et al. (2007). CD8(+) T-cell responses to adeno-associated virus capsid in humans. Nat. Med. *13*, 419–422.

13. Grimm, D., Lee, J.S., Wang, L., Desai, T., Akache, B., Storm, T.A., and Kay, M.A. (2008). In vitro and in vivo gene therapy vector evolution via multispecies interbreeding and retargeting of adeno-associated viruses. J. Virol. *82*, 5887–5911.

14. Li, W., Asokan, A., Wu, Z., Van Dyke, T., DiPrimio, N., Johnson, J.S., Govindaswamy, L., Agbandje-McKenna, M., Leichtle, S., Eugene Redmond, D., Jr., et al. (2008). Engineering and selection of shuffled AAV genomes: a new strategy for producing targeted biological nanoparticles. Mol. Ther. *16*, 1252–1260.

15. Kotterman, M.A., and Schaffer, D.V. (2014). Engineering adeno-associated viruses for clinical gene therapy. Nat. Rev. Genet. *15*, 445–451.

16. Gray, S.J., Blake, B.L., Criswell, H.E., Nicolson, S.C., Samulski, R.J., McCown, T.J., and Li, W. (2010). Directed evolution of a novel adeno-associated virus (AAV) vector that crosses the seizure-compromised blood-brain barrier (BBB). Mol. Ther. *18*, 570–578.

17. Jang, J.H., Koerber, J.T., Kim, J.S., Asuri, P., Vazin, T., Bartel, M., Keung, A., Kwon, I., Park, K.I., and Schaffer, D.V. (2011). An evolved adeno-associated viral variant enhances gene delivery and gene targeting in neural stem cells. Mol. Ther. *19*, 667–675.

18. Davidoff, A.M., Gray, J.T., Ng, C.Y., Zhang, Y., Zhou, J., Spence, Y., Bakar, Y., and Nathwani, A.C. (2005). Comparison of the ability of adeno-associated viral vectors pseudotyped with serotype 2, 5, and 8 capsid proteins to mediate efficient transduction of the liver in murine and nonhuman primate models. Mol. Ther. *11*, 875–888.

19. Nathwani, A.C., Gray, J.T., McIntosh, J., Ng, C.Y., Zhou, J., Spence, Y., Cochrane, M., Gray, E., Tuddenham, E.G., and Davidoff, A.M. (2007). Safe and efficient transduction of the liver after peripheral vein infusion of self-complementary AAV vector results in stable therapeutic expression of human FIX in nonhuman primates. Blood *109*, 1414–1421.

20. Nathwani, A.C., Gray, J.T., Ng, C.Y., Zhou, J., Spence, Y., Waddington, S.N., Tuddenham, E.G., Kemball-Cook, G., McIntosh, J., Boon-Spijker, M., et al. (2006). Self-complementary adeno-associated virus vectors containing a novel liver-specific human factor IX expression cassette enable highly efficient transduction of murine and nonhuman primate liver. Blood *107*, 2653–2661.

21. Salganik, M., Aydemir, F., Nam, H.J., McKenna, R., Agbandje-McKenna, M., and Muzyczka, N. (2014). Adeno-associated virus capsid proteins may play a role in transcription and second-strand synthesis of recombinant genomes. J. Virol. *88*, 1071–1079.

22. Chatterjee, S., Smith, L., and Wong, K. 2015. Adeno-associated virus vector variants for high efficiency genome editing and methods thereof. U.S. patent 62/209,862, filed August 25, 2015, and published July 13, 2017.

23. Xiao, W., Chirmule, N., Berta, S.C., McCullough, B., Gao, G., and Wilson, J.M. (1999). Gene therapy vectors based on adeno-associated virus type 1. J. Virol. *73*, 3994–4003.

24. Zincarelli, C., Soltys, S., Rengo, G., and Rabinowitz, J.E. (2008). Analysis of AAV serotypes 1-9 mediated gene expression and tropism in mice after systemic injection. Mol. Ther. *16*, 1073–1080.

25. Azuma, H., Paulk, N., Ranade, A., Dorrell, C., Al-Dhalimy, M., Ellis, E., Strom, S., Kay, M.A., Finegold, M., and Grompe, M. (2007). Robust expansion of human hepatocytes in Fah-/-/Rag2-/-/Il2rg-/- mice. Nat. Biotechnol. *25*, 903–910.

26. Opie, S.R., Warrington, K.H., Jr., Agbandje-McKenna, M., Zolotukhin, S., and Muzyczka, N. (2003). Identification of amino acid residues in the capsid proteins of adeno-associated virus type 2 that contribute to heparan sulfate proteoglycan binding. J. Virol. *77*, 6995–7006.

27. Turunen, T.A., Kurkipuro, J., Heikura, T., Vuorio, T., Hytönen, E., Izsvák, Z., and Ylä-Herttuala, S. (2016). Sleeping beauty transposon vectors in liver-directed gene delivery of LDLR and VLDLR for gene therapy of familial hypercholesterolemia. Mol. Ther. *24*, 620–635.

28. Calcedo, R., Vandenberghe, L.H., Gao, G., Lin, J., and Wilson, J.M. (2009). Worldwide epidemiology of neutralizing antibodies to adeno-associated viruses. J. Infect. Dis. *199*, 381–390.

29. van der Marel, S., Comijn, E.M., Verspaget, H.W., van Deventer, S., van den Brink, G.R., Petry, H., Hommes, D.W., and Ferreira, V. (2011). Neutralizing antibodies against adeno-associated viruses in inflammatory bowel disease patients: implications for gene therapy. Inflamm. Bowel Dis. *17*, 2436–2442.

30. Wang, L., Bell, P., Somanathan, S., Wang, Q., He, Z., Yu, H., McMenamin, D., Goode, T., Calcedo, R., and Wilson, J.M. (2015). Comparative study of liver gene transfer with AAV vectors based on natural and engineered AAV capsids. Mol. Ther. *23*, 1877–1887.

31. Kay, M.A. (2015). Selecting the best AAV capsid for human studies. Mol. Ther. *23*, 1800–1801.

32. Zen, Z., Espinoza, Y., Bleu, T., Sommer, J.M., and Wright, J.F. (2004). Infectious titer assay for adeno-associated virus vectors with sensitivity sufficient to detect single infectious events. Hum. Gene Ther. *15*, 709–715.

33. Grimm, D., Kern, A., Pawlita, M., Ferrari, F., Samulski, R., and Kleinschmidt, J. (1999). Titration of AAV-2 particles via a novel capsid ELISA: packaging of genomes can limit production of recombinant AAV-2. Gene Ther. *6*, 1322–1330.

34. Calcedo, R., and Wilson, J.M. (2013). Humoral immune response to AAV. Front. Immunol. *4*, 341.

35. Boutin, S., Monteilhet, V., Veron, P., Leborgne, C., Benveniste, O., Montus, M.F., and Masurier, C. (2010). Prevalence of serum IgG and neutralizing factors against adeno-associated virus (AAV) types 1, 2, 5, 6, 8, and 9 in the healthy population: implications for gene therapy using AAV vectors. Hum. Gene Ther. *21*, 704–712.

36. Halbert, C.L., Miller, A.D., McNamara, S., Emerson, J., Gibson, R.L., Ramsey, B., and Aitken, M.L. (2006). Prevalence of neutralizing antibodies against adeno-associated virus (AAV) types 2, 5, and 6 in cystic fibrosis and normal populations: Implications for gene therapy using AAV vectors. Hum. Gene Ther. *17*, 440–447.

37. Han, X., and Ni, W. (2015). Cost-effectiveness analysis of Glybera for the treatment of lipoprotein lipase deficiency. Value Health *18*, A756.

38. Morrison, C. (2015). $1-million price tag set for Glybera gene therapy. Nat. Biotechnol. *33*, 217–218.

39. Mingozzi, F., and High, K.A. (2013). Immune responses to AAV vectors: overcoming barriers to successful gene therapy. Blood *122*, 23–36.

40. Grimm, D. (2002). Production methods for gene transfer vectors based on adeno-associated virus serotypes. Methods *28*, 146–157.

41. Cunningham, S.C., Dane, A.P., Spinoulas, A., Logan, G.J., and Alexander, I.E. (2008). Gene delivery to the juvenile mouse liver using AAV2/8 vectors. Mol. Ther. *16*, 1081–1088.

42. Wilson, E.M., Bial, J., Tarlow, B., Bial, G., Jensen, B., Greiner, D.L., Brehm, M.A., and Grompe, M. (2014). Extensive double humanization of both liver and hematopoiesis in FRGN mice. Stem Cell Res. (Amst.) *13* (3 Pt A), 404–412.

43. Huang, W., Johnston, W.A., Boden, M., and Gillam, E.M. (2016). ReX: a suite of computational tools for the design, visualization, and analysis of chimeric protein libraries. Biotechniques *60*, 91–94.

44. Weirather, J.L., de Cesare, M., Wang, Y., Piazza, P., Sebastiano, V., Wang, X.J., Buck, D., and Au, K.F. (2017). Comprehensive comparison of Pacific Biosciences and Oxford Nanopore Technologies and their applications to transcriptome analysis. F1000Res. *6*, 100.

45. Jiao, X., Zheng, X., Ma, L., Kutty, G., Gogineni, E., Sun, Q., Sherman, B.T., Hu, X., Jones, K., Raley, C., et al. (2013). A benchmark study on error assessment and quality control of CCS reads derived from the PacBio RS. J. Data Mining Genomics Proteomics *4*, 16008.

46. Edgar, R.C. (2004). MUSCLE: multiple sequence alignment with high accuracy and high throughput. Nucleic Acids Res. *32*, 1792–1797.

47. Stamatakis, A., Ludwig, T., and Meier, H. (2005). RAxML-III: a fast program for maximum likelihood-based inference of large phylogenetic trees. Bioinformatics *21*, 456–463.

48. Barzel, A., Paulk, N.K., Shi, Y., Huang, Y., Chu, K., Zhang, F., Valdmanis, P.N., Spector, L.P., Porteus, M.H., Gaensler, K.M., and Kay, M.A. (2015). Promoterless gene targeting without nucleases ameliorates haemophilia B in mice. Nature *517*, 360–364.

49. Namekawa, S.H., Payer, B., Huynh, K.D., Jaenisch, R., and Lee, J.T. (2010). Two-step imprinted X inactivation: repeat versus genic silencing in the mouse. Mol. Cell. Biol. *30*, 3187–3205.

50. Huch, M., Dorrell, C., Boj, S.F., van Es, J.H., Li, V.S., van de Wetering, M., Sato, T., Hamer, K., Sasaki, N., Finegold, M.J., et al. (2013). In vitro expansion of single Lgr5+ liver stem cells induced by Wnt-driven regeneration. Nature *494*, 247–250.

51. Dorrell, C., Tarlow, B., Wang, Y., Canaday, P.S., Haft, A., Schug, J., Streeter, P.R., Finegold, M.J., Shenje, L.T., Kaestner, K.H., and Grompe, M. (2014). The organoid-initiating cells in mouse pancreas and liver are phenotypically and functionally similar. Stem Cell Res. (Amst.) *13*, 275–283.

52. Mingozzi, F., Chen, Y., Edmonson, S.C., Zhou, S., Thurlings, R.M., Tak, P.P., High, K.A., and Vervoordeldonk, M.J. (2013). Prevalence and pharmacological modulation of humoral immunity to AAV vectors in gene transfer to synovial tissue. Gene Ther. *20*, 417–424.

53. Meliani, A., Leborgne, C., Triffault, S., Jeanson-Leh, L., Veron, P., and Mingozzi, F. (2015). Determination of anti-adeno-associated virus vector neutralizing antibody titer with an in vitro reporter system. Hum. Gene Ther. Methods *26*, 45–53.

54. Xie, Q., Bu, W., Bhatia, S., Hare, J., Somasundaram, T., Azzi, A., and Chapman, M.S. (2002). The atomic structure of adeno-associated virus (AAV-2), a vector for human gene therapy. Proc. Natl. Acad. Sci. USA *99*, 10405–10410.

55. Dane, A.P., Wowro, S.J., Cunningham, S.C., and Alexander, I.E. (2013). Comparison of gene transfer to the murine liver following intraperitoneal and intraportal delivery of hepatotropic AAV pseudo-serotypes. Gene Ther. *20*, 460–464.

56. Li, S., Ling, C., Zhong, L., Li, M., Su, Q., He, R., Tang, Q., Greiner, D.L., Shultz, L.D., Brehm, M.A., et al. (2015). Efficient and targeted transduction of nonhuman primate liver with systemically delivered optimized AAV3B vectors. Mol. Ther. *23*, 1867–1876.

57. D'Avola, D., López-Franco, E., Sangro, B., Pañeda, A., Grossios, N., Gil-Farina, I., Benito, A., Twisk, J., Paz, M., Ruiz, J., et al. (2016). Phase I open label liver-directed gene therapy clinical trial for acute intermittent porphyria. J. Hepatol. *65*, 776–783.

58. uniQure. December 3, 2016. Press release: uniQure announces first clinical data from second dose cohort of AMT-060 in ongoing phase I/II trial in patients with severe hemophilia B. https://globenewswire.com/news-release/2016/12/03/894861/0/en/uniQure-Announces-First-Clinical-Data-From-Second-Dose-Cohort-of-AMT-060-in-Ongoing-Phase-I-II-trial-in-Patients-with-Severe-Hemophilia-B.html.

59. Pañeda, A., Vanrell, L., Mauleon, I., Crettaz, J.S., Berraondo, P., Timmermans, E.J., Beattie, S.G., Twisk, J., van Deventer, S., Prieto, J., et al. (2009). Effect of adeno-associated virus serotype and genomic structure on liver transduction and biodistribution in mice of both genders. Hum. Gene Ther. *20*, 908–917.

60. Nakai, H., Fuess, S., Storm, T.A., Muramatsu, S., Nara, Y., and Kay, M.A. (2005). Unrestricted hepatocyte transduction with adeno-associated virus serotype 8 vectors in mice. J. Virol. *79*, 214–224.